Thermodynamic Modeling of Copper Ore Treating into Matte Using Borate Containing Materials

Alexander Akberdin
Zh. Abishev Chemical-Metallurgical Institute, Karaganda, Kazakhstan
akberdin_38@mail.ru

Alexander Kim
Zh. Abishev Chemical-Metallurgical Institute, Karaganda, Kazakhstan
boron_213@mail.ru

Ruslan Sultangaziyev
Abylkas Saginov Karaganda Technical University, Karaganda, Kazakhstan | Zh. Abishev Chemical-Metallurgical Institute, Karaganda, Kazakhstan
sulrus83@mail.ru (corresponding author)

Alexey Orlov
Zh. Abishev Chemical-Metallurgical Institute, Karaganda, Kazakhstan
wolftailer@mail.ru

Anel Jashibekova
Abylkas Saginov Karaganda Technical University, Karaganda, Kazakhstan | Zh. Abishev Chemical-Metallurgical Institute, Karaganda, Kazakhstan
anelyadzhashi@gmail.com

Received: 10 April 2025 | Revised: 16 May 2025 | Accepted: 24 May 2025

 DOI: https://doi.org/10.48084/etasr.11401

ABSTRACT

This work examines the possibility of incorporating borate-containing materials in order to improve the granule strength and reduce the copper losses to slag. A phase diagram of the Fe-S-Cu system was constructed, and a mathematical model with a numerical calculation program were created. Using complete thermodynamic modeling, the influence of the boric anhydride and borate ore on the pelletizing, drying, roasting, and matte production was analyzed. B_2O_3 enhanced the wet granule strength by forming crystalline hydrates ($H_2O \cdot B_2O_3$), which dehydrated at 285 K and melted at 723 K, creating a strong sinter upon cooling. During smelting, boron-containing materials increased process efficiency and they decreased matte losses, creating low-melting, mobile slags. Additionally, borate ore containing montmorillonite ensured sufficient wet granule strength for transport, and its low-melting nature led to liquid phase formation during firing, producing a strong sinter upon cooling.

Keywords-thermodynamic modeling; copper ore; granules; drying; roasting; matte

I. INTRODUCTION

Copper pyrometallurgy presents a number of challenges mainly related to the agglomeration of finely ground concentrates. Lignosulfonate, which is widely used for this purpose, does not completely address issues, such as the removal of materials from the smelting furnace and loss of copper in the slag. Several studies have examined new effective flux additives to improve the quality of copper granules. For example, attempts have been made to replace part of the lignosulfonate with copper sulfate [1] as well as with a solution of halite (sodium chlorite) [2-4], which did not yield the desired results in increasing the compressive and impact strength of the granules. Other studies have investigated the complete or partial replacement of lignosulfonate with sulfuric acid [5-7] to sulfidize the copper minerals. However, the

findings indicated no significant advantages in the granule strength and raised concerns due to equipment corrosion. Thus, the issue of finding effective flux additives to enhance the quality of copper granules remains relevant. This study aims to identify an additive that can simultaneously improve the granule strength and reduce the copper losses to slag. For this purpose, boric anhydride and natural ores containing it were examined.

II. RESEARCH METHOD

This study considered the application of boric anhydride and naturally occurring boron ores as possible additives to cooper concentrates. The choice of these materials was based on an experimentally found effect on blast furnace, steelmaking, and ferroalloy slags, where the addition of boron oxide led to a decrease in viscosity, crystallization temperature, density, and surface tension. A complete thermodynamic modeling of the pelletization, drying, roasting, and matte production processes was conducted. The modeling aimed to provide scientific substantiation for the proposed use of borate additives and to predict their influence on phase formation and system behavior under industrial conditions. A diagram of the phase composition of the Fe-S-Cu system as well as its mathematical model were developed. To achieve this, the triangulation method was utilized in which the diagram is represented as a set of elementary triangles of coexisting phases [8-10].

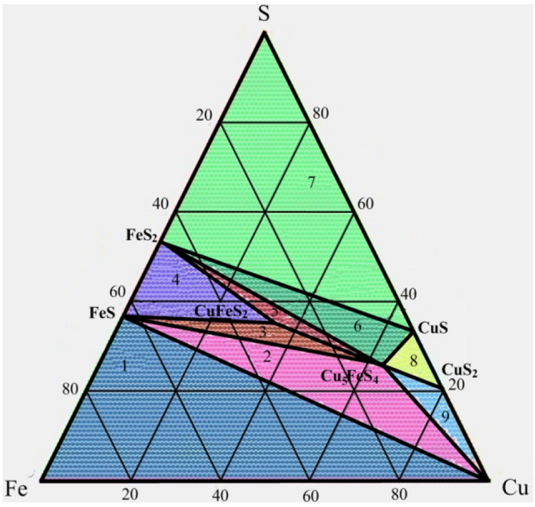

Fig. 1. Diagram of the phase composition of the Fe-S-C system.

Figure 1 illustrates the resulting phase diagram for the system under exploration, which consisted of nine triangles of coexisting phases:

1. Cu-Fe-FeS,
2. Cu-Cu_5FeS_4-FeS,
3. $CuFeS_2$-Cu_5FeS_4-FeS,
4. $CuFeS_2$-Cu_5FeS_4-FeS_2,
5. Cu_5FeS_4-CuS-FeS_2,
6. S-CuS-FeS_2,
7. Cu_5FeS_4-CuS-Cu_2S,
8. Cu-Cu_5FeS_4-Cu_2S,
9. FeS-FeS_2-$CuFeS_2$.

III. RESULTS AND DISCUSSION

From the resulting diagram, the phase composition of the concentrate based on its main elements was determined according to the rule of segments [11], which involves plotting its chemical composition onto the phase diagram. To facilitate these calculations, a mathematical model of the diagram was developed using a previously established method [12]. Such a model was created for each elementary triangle in the form of equations for the dependence of the phase composition of the concentrate on its chemical composition (Cu_0, S_0, Fe_0). The resulting equations for all elementary triangles are presented in Table I.

TABLE I. SUMMARY CHARACTERISTICS OF THE FE-S-CU SYSTEM

No	Triangle	Transformation equations	Area, *S*, (m^2)
1	Cu-Fe-FeS	$Cu = Cu_0$ $Fe = Fe_0 - 1.741 \cdot S_0$ $FeS = 2.741 \cdot S_0$	0.1579
2	Cu-Cu_5FeS_4-FeS	$Cu = Cu_0 + 1.897 \cdot Fe_0 - 3.303 \cdot S_0$ $Cu_5FeS_4 = -2.996 \cdot Fe_0 + 5.219 \cdot S_0$ $FeS = 2.099 \cdot Fe_0 - 0.914 \cdot S_0$	0.0527
3	$CuFeS_2$-Cu_5FeS_4-FeS	$CuFeS_2 = -4.321 \cdot Cu_0 - 8.198 \cdot Fe_0 + 14.282 \cdot S_0$ $Cu_5FeS_4 = 3.942 \cdot Cu_0 + 4.483 \cdot Fe_0 - 7.810 \cdot S_0$ $FeS = 1.379 \cdot Cu_0 + 4.715 \cdot Fe_0 - 5.472 \cdot S_0$	0.0122
4	$CuFeS_2$-Cu_5FeS_4-FeS_2	$CuFeS_2 = 2.891 \cdot Cu0 + 16.463 \cdot Fe0 - 14.338 \cdot S_0$ $Cu_5FeS_4 = -0.02 \cdot Cu_0 - 9.003 \cdot Fe_0 + 7.841 \cdot S_0$ $FeS_2 = -1.889 \cdot Cu_0 - 6.460 \cdot Fe_0 + 7.497 \cdot S_0$	0.0089
5	Cu_5FeS_4-CuS-FeS_2	$Cu_5FeS_4 = 2.631 \cdot Cu_0 + 5.989 \cdot Fe_0 - 5.216 \cdot S_0$ $CuS = -1.002 \cdot Cu_0 - 5.705 \cdot Fe_0 + 4.969 \cdot S_0$ $FeS_2 = -0.629 \cdot Cu_0 + 0.716 \cdot Fe_0 + 1.247 \cdot S_0$	0.0257
6	S-CuS-FeS_2	$S = -0.504 \cdot Cu_0 - 1.148 \cdot Fe_0 + S_0$ $CuS = 1.504 \cdot Cu_0$ $FeS_2 = 2.148 \cdot Fe_0$	0.1340
7	Cu_5FeS_4-CuS-Cu_2S	$Cu_5FeS_4 = 8.984 \cdot Fe_0$ $CuS = -1.504 \cdot Cu_0 - 5.134 \cdot Fe_0 + 5.964 \cdot S_0$ $Cu_2S = 2.504 \cdot Cu_0 - 2.850 \cdot Fe_0 - 4.964 \cdot S_0$	0.0064
8	Cu-Cu_5FeS_4-Cu_2S	$Cu = Cu_0 + 3.413 \cdot Fe_0 - 3.965 \cdot S_0$ $Cu_5FeS4 = 8.985 \cdot Fe_0$ $Cu_2S = -11.398 \cdot Fe_0 + 4.965 \cdot S_0$	0.0097
9	FeS-FeS_2-$CuFeS_2$	$FeS = -0.00004 \cdot Cu_0 + 3.147 \cdot Fe_0 - 2.741 \cdot S$ $FeS_2 = -1.88762 \cdot Cu_0 - 2.147 \cdot Fe_0 + 3.741 \cdot S_0$ $CuFeS_2 = 2.88766 \cdot Cu_0$	0.0255

The area of each triangle (*S*) is also included in Table I. Among them, Triangle 1 exhibited the largest area, while Triangle 7 had the smallest. A larger area indicates a broader compositional stability range. Therefore, operating within Triangle 1 ensures more stable process performance, even in the presence of inevitable fluctuations in the chemical composition of the incoming materials-provided that this region also meets process manufacturability requirements.

A computer program was created in order to automate these equations (Figure 2). After inputting the chemical composition of copper ore or concentrate through the console, the program identifies the elementary triangle and calculates its phase composition in mass percent. This tool accelerates the quantitative assessment of the phase composition of various copper raw materials based on their main elements. An example of model usage is presented in Table II after recalculating Cu, Fe, and S concentrations to 100% (numbers in parentheses) [5].

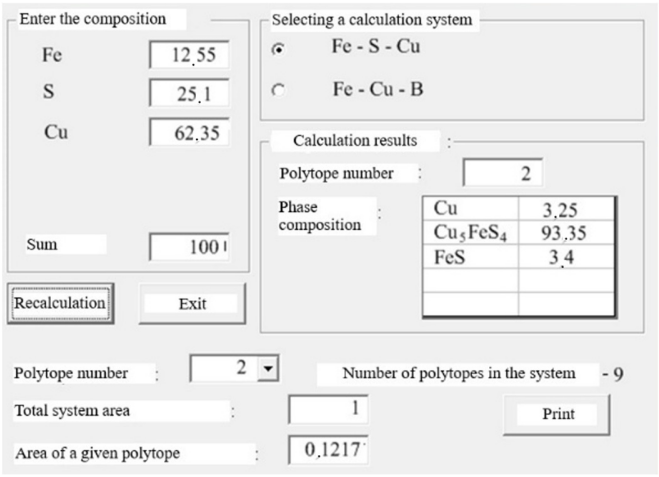

Fig. 2. Computer program window.

TABLE II. CHEMICAL AND PHASE COMPOSITION OF CONCENTRATES [5]

Concentrates Kazakhstan	Element content. wt.%			Phase content (wt.%)		
	Cu	Fe	S			
Zhezkazgan	35.4 (59.3)	7.72 (12.9)	16.6 (27.8)	Cu	Cu_5FeS_4	FeS
				88.33	5.03	6.63
Nurkazgan	21.7 (28.1)	24.5 (31.8)	30.94 (40.1)	$CuFeS_2$	Cu_5FeS_4	FeS_2
				29.09	28.00	42.39
Balkhash	21.74 (28.3)	28.9 (37.7)	26.1 (34.0)	$CuFeS_2$	Cu_5FeS_4	FeS_2
				54.58	14.88	30.53
Mixture	32.85 (52.3)	11.57 (18.4)	18.39 (29.3)	Cu_5FeS_4	CuS	FeS_2
				34.63	62.7	1.72

The calculated results showed a good agreement with those determined experimentally [13-16]. Real concentrates, in addition to Fe, S, and Cu, also contained zinc, lead, calcium oxides, silicon, and other compounds. Therefore, a correct theoretical assessment of the processing of concentrates into final products (pellets, matte, slag) was carried out considering the chemical interaction of all components with each other.

This opportunity can be provided by special thermodynamic complexes [17]. In this work, the TERRA software package was employed [18, 19]. The advantage of this approach was not only including all components of the initial concentrate, adding fluxes, and reducing agents, but also setting the temperature and the desired gas phase in the unit used. This enabled an accurate prediction of the compositions of both resulting condensed products and the released gases, which is important for optimizing the environmental requirements.

Based in these calculations, a list of possible condensed and gaseous phases during the processing of the copper ore concentrate was established. Their thermochemical characteristics, such as enthalpy of formation, enthalpy increment, entropy at 298 K, temperature dependence of heat capacity, and others were entered into the thermodynamic database of TERRA. The dynamics of the phase changes over the temperature range of 300-1600 K were examined for the Zhezkazgan concentrate containing 39.5% Cu, 15.9% S, 7.95% Fe, 0.91% Zn, 1.96% Pb, 19, 1% SiO_2, and 1.9% CaO, rounded with industrial water as a binder. For convenience, the matte, slag, and steam-gas parts were identified (Figures 3-4).

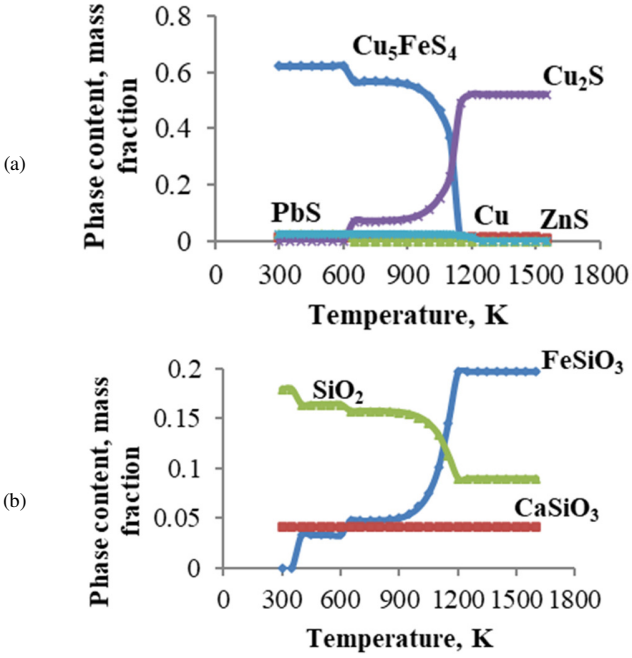

Fig. 3. Phase composition of: (a) matte and (b) slag part of granules, rounded with technical water.

The dominant phase of the pelletized concentrate was bornite (Cu_5FeS_4). It also contained zinc (ZnS) and lead (PbS) sulfides (Figure 3(a)). Due to sulfur deficiency, the formation of metallic copper (Cu) occurred in the matte, which was also predicted by the earlier modeling calculations of the Fe-S-Cu system.

The slag phase was mainly composed of silica (SiO_2), iron monosilicate ($FeSiO_3$), magnetite (Fe_3O_4), and wollastonite ($CaSiO_3$) (Figure 3(b)). Under the equilibrium conditions

formed by the TERRA software, no copper compounds were present in the slag.

Like any substance, a vapor-gas phase was formed above the concentrate (Figure 4). This was mainly water vapor (H_2O) from the process, water used for pelletizing, hydrogen sulfide, as well as sulfur and its oxides.

Noticeable changes in the granules prepared from the concentrate were observed during the process of heating them for drying and firing. Starting from 650 K, the amount of Cu_5FeS_4 in the matte part started to fall with the simultaneous appearance of Cu_2S here and S_2 in the gas. At 1150 K, Cu_5FeS_4 completely disappeared, while chalcopyrite $CuFeS_2$ appeared with a further increase in the Cu_2S content.

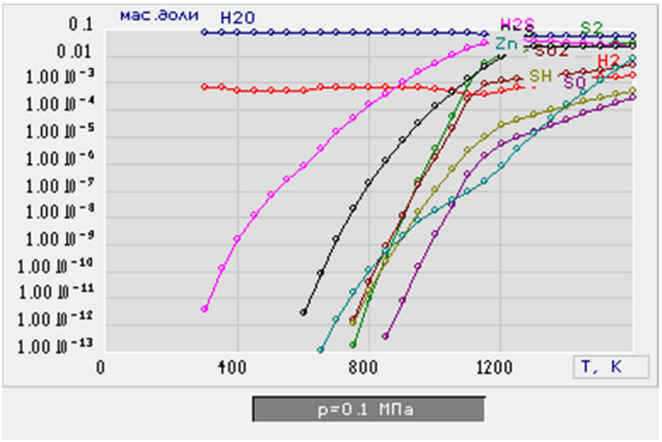

Fig. 4. Phase composition of gas above the concentrate, rounded using technical water.

This transition can be described schematically as follows:

$$Cu_5FeS_4 \rightarrow CuFeS_2 + Cu_2S$$

Starting at 1200 K, the matte part of the granules mostly consisted of Cu_2S, along with small amounts of FeS, PbS, and ZnS formed as a result of the transformation described by the reaction:

$$CuFeS_2 = 2Cu_2S + 4FeS + S_2$$

B_2O_3 was tested as a binder in the production of granules instead of industrial water. Its consumption was set in the range of 0.5-5 % of the concentrate weight (Figures 5 and 6). It can be observed that even at the imbrication stage (300 K), the interaction of B_2O_3 with the moisture of the concentrate led to the formation of sassolite ($H_2O{\cdot}B_2O_3$). According to the experience of pelletizing iron ore concentrates, the resulting sassolite crystals are known to increase their strength, reducing the need for regranulation due to fragmentation during the transportation of wet granules from the pelletizing shop to the roasting unit. The matte part of the granules was isolated (Figure 6) revealing no significant changes when compared with the granules made using water as a binder.

When the granules were heat treated reaching 285 K, sassolite lost water, turning back into boron oxide. It was assumed that it could give the compound CuB_2O_4 with copper oxide by changing the matte part of the granules. Instead, thermodynamic modeling revealed that B_2O_3 preferred to react not with CuO (Figure 7), but with a stronger base, such as CaO (Figure 8).

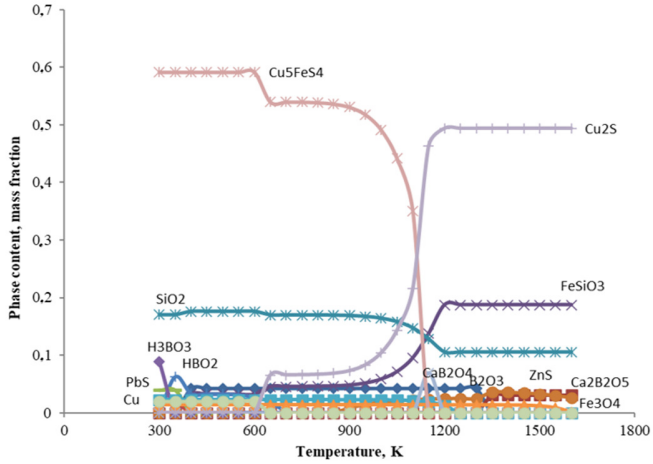

Fig. 5. Effect of 5 % B_2O_3 on the phase composition of granules in the temperature range of 300-1600 K.

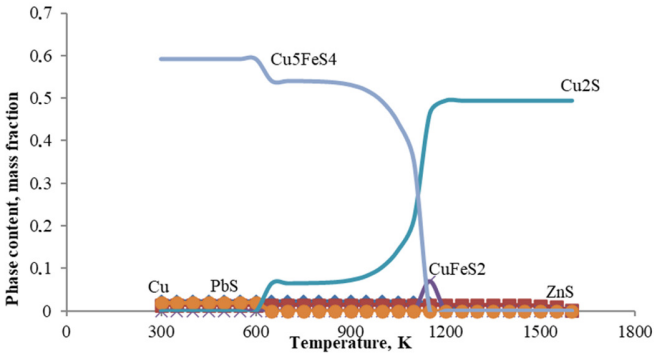

Fig. 6. Phase composition of the matte part of granules with 5 % B_2O_3.

	T	Cp	H	S	G	Reference
1	1CuO + 1B2O3 = 1CuB2O4					
2	T	deltaH	deltaS	deltaG	K	Log(K)
3	K	kJ	J/K	kJ		
4	273,000	-1,643	-15,305	2,535	3,273E-001	-0,485
5	373,000	4,175	3,003	3,055	3,734E-001	-0,428
6	473,000	8,580	13,516	2,187	5,735E-001	-0,241
7	573,000	12,074	20,240	0,476	9,049E-001	-0,043
8	673,000	14,942	24,866	-1,792	1,378E+000	0,139
9	773,000	-7,757	-6,471	-2,755	1,535E+000	0,186
10	873,000	-7,342	-5,969	-2,131	1,341E+000	0,128
11	973,000	-6,641	-5,212	-1,570	1,214E+000	0,084
12	1073,000	-5,650	-4,245	-1,095	1,131E+000	0,053
13	1173,000	-4,363	-3,100	-0,727	1,077E+000	0,032
14	1273,000	-2,778	-1,805	-0,480	1,046E+000	0,020
15	1373,000	-0,893	-0,381	-0,370	1,033E+000	0,014
16	1473,000	1,295	1,156	-0,408	1,034E+000	0,014
17	1573,000	3,785	2,791	-0,605	1,047E+000	0,020
18	1673,000	6,580	4,512	-0,969	1,072E+000	0,030
19	1773,000	9,679	6,310	-1,510	1,108E+000	0,044
20	1873,000	13,083	8,177	-2,233	1,154E+000	0,062

Exit | Help | Print | Clear | Copy All | Copy | Save

Fig. 7. Thermodynamics of copper borate formation.

	T	Cp	H	S	G	Reference
1	1CaO + 1B2O3 = 1CaB2O4					
2	T	deltaH	deltaS	deltaG	K	Log(K)
3	K	kJ	J/K	kJ		
4	273.000	-123.868	13.054	-127.432	2.422E+024	24.384
5	373.000	-123.975	12.689	-128.709	1.061E+018	18.026
6	473.000	-124.012	12.608	-129.976	2.263E+014	14.355
7	573.000	-124.223	12.210	-131.219	9.182E+011	11.963
8	673.000	-124.625	11.566	-132.409	1.896E+010	10.278
9	773.000	-150.310	-23.910	-131.828	8.107E+008	8.909
10	873.000	-152.672	-26.789	-129.285	5.448E+007	7.736
11	973.000	-154.590	-28.873	-126.496	6.186E+006	6.791
12	1073.000	-156.085	-30.339	-123.531	1.033E+006	6.014
13	1173.000	-157.174	-31.312	-120.445	2.312E+005	5.364
14	1273.000	-157.866	-31.880	-117.282	6.498E+004	4.813
15	1373.000	-158.168	-32.111	-114.080	2.190E+004	4.340
16	1473.000	-81.205	21.570	-112.978	1.016E+004	4.007
17	1573.000	-73.980	26.316	-115.375	6.785E+003	3.832
18	1673.000	-66.805	30.738	-118.230	4.917E+003	3.692
19	1773.000	-59.677	34.876	-121.513	3.804E+003	3.580
20	1873.000	-52.597	38.761	-125.197	3.103E+003	3.492

Exit Help Print Clear Copy All Copy Save

Fig. 8. Thermodynamics of calcium borate formation.

As a result, calcium borates CaB_2O_4 and $Ca_2B_2O_5$ appeared, turning into slag (Figure 9). They reduced not only the viscosity, but also the surface tension of the slags [20-21]. These factors contributed to the merging of matte particles and increasing the rate of their settling from the slag. The slag also contained silica (SiO_2), iron monosilicate ($FeSiO_3$), wollastonite ($CaSiO_3$), and magnetite (Fe_3O_4).

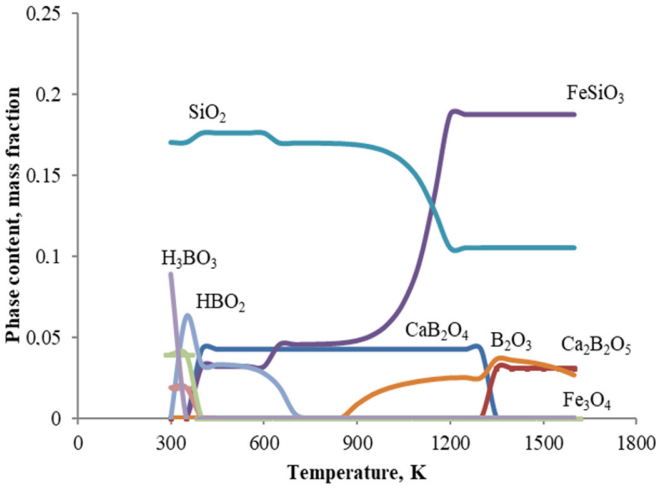

Fig. 9. Phase composition of the slag part of granules with 5% B_2O_3.

In Kazakhstan there are borate ores, the average chemical composition of which can be characterized by the following data: 8.52 wt.% CaO, 9.8 wt.% MgO, 14.71 wt.% SiO_2, 1.65 wt.% Al_2O_3, 7.58 wt.% B_2O_3, 1.48 wt.% Fe_2O_3, 35.05 wt.% $CaSO_4$, and 21.21 wt.% H_2O. Their distinctive feature is the presence of montmorillonite, which is the main component of bentonites, allowing one to count on the manifestation of clumping properties by the ore. The melting temperature of ores is in the range of 1373-1473 K, and the viscosity at complete melting is 0.3-0.5 Pa·s.

Figures 10 and 11 present the effect of additives of 5% of this ore on the phase composition of granules from the copper ore concentrate.

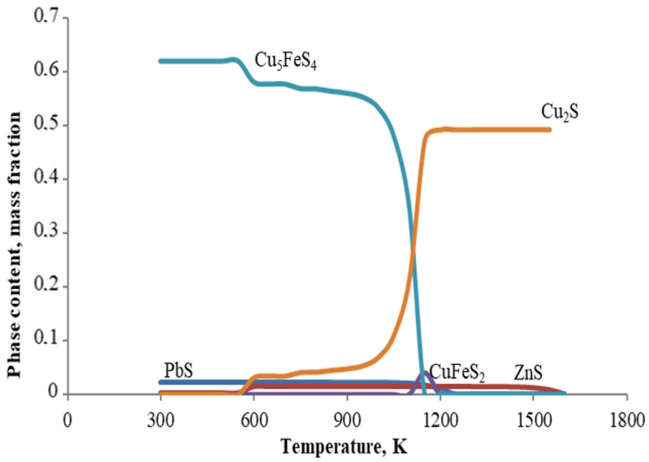

Fig. 10. Phase composition of the matte part of the granules with the addition of 5% Inder borate ore.

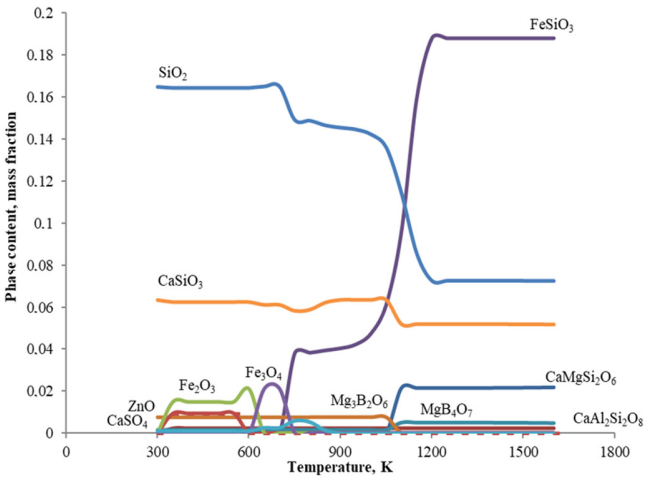

Fig. 11. Phase composition of the slag part of the granules with the addition of 5% Inder borate ore.

The matte part was dominated by Cu_5FeS_4 and Cu_2S. At 1150 K, Cu_5FeS_4 disappeared, $CuFeS_2$ appeared, and the amount of Cu_2S increased. Above 1200 K, the matte contained Cu_2S, PbS, and ZnS (Figure 10).The slag part was composed of tridymite (SiO_2), iron monosilicate ($FeSiO_3$), wollastonite ($CaSiO_3$), magnetite (Fe_3O_4), diopside ($CaMgSi_2O_8$), magnesium borates ($Mg_3B_2O_6$, MgB_4O_7), and calcium sulfate ($CaSO_4$). The influx of calcium oxide was sufficient not only for the formation of $CaSiO_3$ and $CaMgSi_2O_8$, but also of a small amount of anorthite ($CaAl_2Si_2O_8$) (Figure 11). Up to 600 K, zinc oxide (ZnO) was present in the slag.

The dynamic behavior of the phase changes of granules with an increase in the consumption of borate ore to 10% of the concentrate weight is displayed in Figures 12 and 13.The matte part of the granules was formed by Cu_5FeS_4, Cu_2S, PbS, and ZnS, while chalcopyrite ($CuFeS_2$) was absent (Figure 12). The slag was characterized by an increased content of effective thinners ($Mg_3B_2O_6$, MgB_4O_7) and anhydride ($CaSO_4$), which is a product of the transformation of gypsum ($CaSO_4 \cdot 2H_2O$).

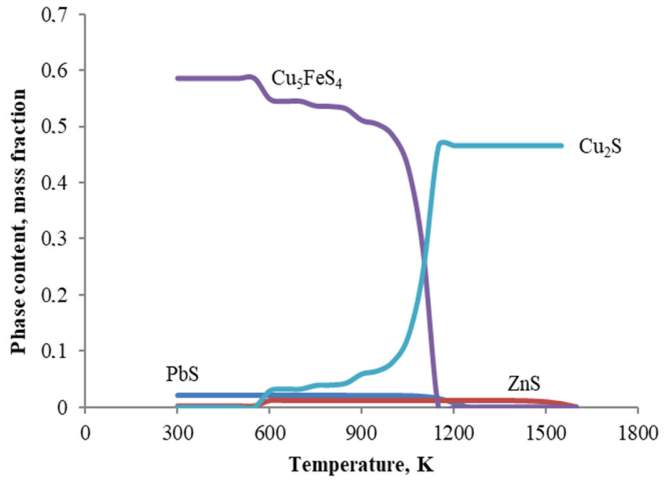

Fig. 12. Phase composition of the matte part of the granules with the addition of 10 % Inder borate ore.

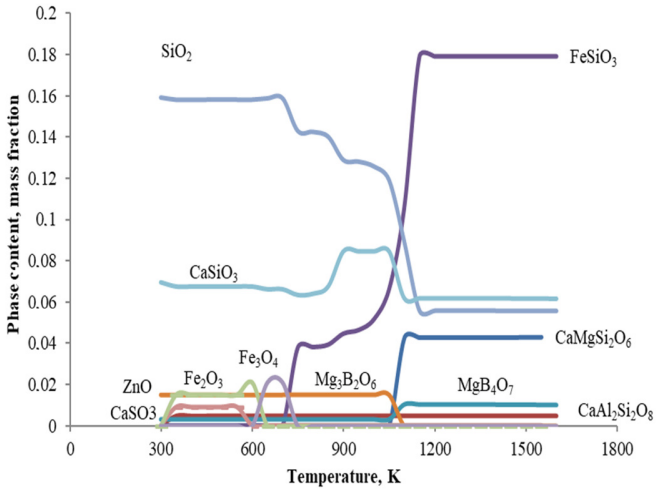

Fig. 13. Phase composition of the slag part of the granules with the addition of 10% Inder borate ore.

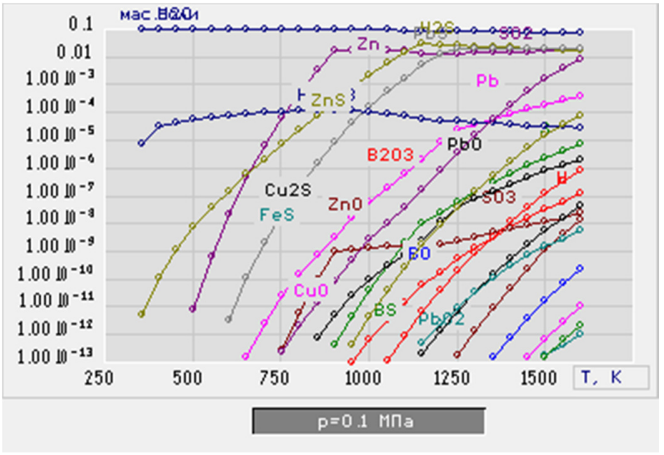

Fig. 14. Composition of the gas phase above granules with an additive of 10% Inder borate ore.

In the gas phase, an increased amount of water vapor was detected from the hydration water of borate ore (21.21%) and the process water used for pelletizing the concentrate (8%). The gas also included oxides and sulfides of zinc, copper, lead, and boron (Figure 14).

IV. CONCLUSION

This study investigated the potential of boron-containing additives to enhance the performance of copper ore concentrates during pelletizing and smelting. A phase composition diagram for the Fe-S-Cu system was constructed, and a mathematical model with a computer program for numerical calculations of the phase composition was developed. Using complete thermodynamic modeling, the effects of boric anhydride and borate ore on each process were analyzed. The results demonstrated that the addition of B_2O_3 and borate ore enhanced the wet granule through the formation of crystalline hydrates ($H_2O \cdot B_2O_3$), which dehydrated at approximately 285 K and melted at 723 K. During smelting, boron-containing materials improved process efficiency and reduced matte losses by forming low-melting, mobile slags. Similarly, borate ore containing montmorillonite ensured sufficient wet granule strength for transport. Its low-melting nature led to liquid phase formation during firing, producing a strong sinter upon cooling. In summary, both B_2O_3 and borate ore are promising additives for copper concentrate processing, improving its overall performance, offering a dual benefit of mechanical strength and metallurgical efficiency.

ACKNOWLEDGMENT

This research is funded by the Science Committee of the Ministry of Education and Science of the Republic of Kazakhstan (Grant No. AP19676780).

REFERENCES

[1] L. M. Karimova, Y. T. Kairalapov, and V. O. Bukharitsin, "Differential thermal analysis of the pelleted rough copper sulphide concentrate of off-balance ore," *Vestnik of Nosov Magnitogorsk State Technical University*, vol. 14, pp. 12–17, Jan. 2016, https://doi.org/10.18503/1995-2732-2016-14-1-12-17.

[2] I. Volokitina *et al.*, "Study of changes in microstructure and metal interface Cu/Al during bimetallic construction wire straining," *Case Studies in Construction Materials*, vol. 18, Jul. 2023, Art. no. e02162, https://doi.org/10.1016/j.cscm.2023.e02162.

[3] A. Kolesnikov *et al.*, "Processing of Waste from Enrichment with the Production of Cement Clinker and the Extraction of Zinc," *Materials*, vol. 15, no. 1, Jan. 2022, Art. no. 324, https://doi.org/10.3390/ma15010324.

[4] A. Kolesnikov *et al.*, "Modeling of Non-Ferrous Metallurgy Waste Disposal with the Production of Iron Silicides and Zinc Distillation," *Materials*, vol. 15, no. 7, Jan. 2022, Art. no. 2542, https://doi.org/10.3390/ma15072542.

[5] A. V. Klyuev *et al.*, "Experimental studies of the processes of structure formation of composite mixtures with technogenic mechanoactivated silica component," *Construction Materials and Products*, vol. 6, no. 2, pp. 5–18, 2023, https://doi.org/10.58224/2618-7183.

[6] A. Klyuev *et al.*, "Alkali-activated binders based on technogenic fibrous waste," *Case Studies in Construction Materials*, vol. 18, Jul. 2023, Art. no. e02202, https://doi.org/10.1016/j.cscm.2023.e02202.

[7] S. I. Aminjanova, M. I. Muratova, S. B. Mirzajonova, T. P. Karimova, and M. S. Saidova, "Research of Sulfuric Acid Leaching of Copper Off-Balance Ores," *International Journal of Engineering and Advanced*

Technology (IJEAT), vol. 9, no. 2, pp. 813–816, Dec. 2019, https://doi.org/10.35940/ijeat.B3838.129219.

[8] V. V. Lychagin, "On Thermodynamics of Multicomponent Systems," *Lobachevskii Journal of Mathematics*, vol. 44, no. 9, pp. 3952–3962, Sep. 2023, https://doi.org/10.1134/S1995080223090226.

[9] A. S. Kolesnikov, V. N. Naraev, M. I. Natorhin, A. A. Saipov, and O. G. Kolenikova, "Review of the processing of minerals and technologic sulfide raw material with the extraction of metals and recovering elemental sulfur by electrochemical methods," *Rasayan Journal of Chemistry*, vol. 13, no. 4, pp. 2420–2428, 2020.

[10] A. S. Kolesnikov, "Thermodynamic simulation of silicon and iron reduction and zinc and lead distillation in zincoligonite ore-carbon systems," *Russian Journal of Non-Ferrous Metals*, vol. 55, no. 6, pp. 513–518, Nov. 2014, https://doi.org/10.3103/S1067821214060121.

[11] T. B. Massalski, H. Okamoto, P. R. Subramanian, and L. Kacprzak, *Binary Alloy Phase Diagrams, 2nd Edition*, 2nd ed. Detroit, MI, USA: ASM International, 1990.

[12] A. A. Akberdin, A. S. Kim, R. B. Sultangaziev, and A. S. Orlov, "The method of mathematical description of the phase composition diagrams," *CIS Iron Steel Rev*, vol. 25, pp. 79–83, 2023.

[13] S. M. Kozhakhmetov, S. A. Kvyatkovsky, M. K. Sultanov, Z. K. Tulegenova, and A. S. Semenova, "Processing of oxidized copper ores and sulfide copper concentrates of the Actogay deposit by pyrometallurgical methods," *Complex use of mineral resources*, vol. 306, no. 3, pp. 54–62, Aug. 2018, https://doi.org/10.31643/2018/6445.17.

[14] A. K. Serikbayeva, K. Z. Zhumashev, F. A. Berdikulova, and S. K. Akilbekova, "Study of Phase Transformations in Oxidized Copper Ore – Sulfur System," *Izvestiya. Non-Ferrous Metallurgy*, no. 5, pp. 34–41, Nov. 2017, https://doi.org/10.17073/0021-3438-2017-5-34-41.

[15] N. V. Marchenko, "Metallurgy of heavy non-ferrous metals [Electronic resource]: electron. study Manual," *NV Marchenko, EP Vershinina, EM Hildebrandt.–Electron data.(6 MB).–Krasnoyarsk: IPK SFU*, pp. 9–15, 2009.

[16] N. I. Utkin, " Manufacture of Nonferrous Metals," *Russian Journal of Applied Chemistry,* vol. **7**4, no. 11, 2001, Art. no. 1916, https://doi.org/10.1023/A:1017450324057

[17] H. Y. Sohn, "Chapter 2.4 - Process Modeling in Non-Ferrous Metallurgy," in *Treatise on Process Metallurgy*, S. Seetharaman, Ed. Amsterdam, Netherlands: Elsevier, 2014, pp. 701–838.

[18] A. Roine*, HSC 6.0 Chemistry. Chemical reactions and Equilibrium software with extensive thermochemical database and Flowsheet simulation*, 2006.

[19] A. A. Akberdin, A. S. Kim, A. S. Orlov, and R. B. Sultangaziyev, "Mathematical model of the diagram of the Fe-Si-B composition system," *Metalurgija*, vol. 61, no. 1, pp. 182–184, Jan. 2022.

[20] O. Sivrikaya and A. I. Arol, "Use of boron compounds as binders in iron ore pelletization," *Open Mineral Processing Journal*, vol. 3, no. 1, pp. 25–35, 2010.

[21] A. V. Vanyukov and V. Y. Zaitsev, "Slags and mattes of nonferrous metallurgy," *Metallurgy*, 1969.